Reports

A designed, phase changing RTX-based peptide for efficient bioseparations

Oren Shur[1], Kevin Dooley[1], Mark Blenner[2], Matthew Baltimore[1], and Scott Banta[1]
[1]*Department of Chemical Engineering, Columbia University, New York, New York and* [2]*Department of Chemical and Biomolecular Engineering, Clemson University, Clemson, South Carolina*

BioTechniques 54:197-206 (April 2013) doi 10.2144/000114010
Keywords: repeat-in-toxin domain; beta roll domain; stimulus-responsive peptides; precipitation

Supplementary material for this article is available at www.BioTechniques.com/article/114010.

Typically, chromatography is the most costly and time-consuming step in protein purification. As a result, alternative methods have been sought for bioseparations, including the use of stimulus-responsive tags that can reversibly precipitate out of solution in response to the appropriate stimulus. While effective, stimulus-responsive tags tend to require temperature changes or relatively harsh buffer conditions to induce precipitation. Here we describe a synthetic peptide, based on the natural repeat-in-toxin (RTX) domain that undergoes gentler calcium-responsive, reversible precipitation. When coupled to the maltose binding protein (MBP), our calcium-responsive tag efficiently purified the fusion protein. Furthermore, when the MBP was appended to green fluorescent protein (GFP), β-lactamase, or a thermostable alcohol dehydrogenase (AdhD), these constructs could also be purified by calcium-induced precipitation. Finally, protease cleavage of the precipitating tag enables the recovery of pure and active target protein by cycling precipitation before and after cleavage.

Non-chromatographic purification techniques are of significant interest since chromatography is typically the most expensive step in protein purification (1). Alternative approaches often rely on targeted precipitation of the protein of interest. One approach is metal chelate affinity precipitation, where thermoresponsive copolymers can be used to specifically precipitate out poly-histidine tagged recombinant proteins (2,3). Another purely protein-based approach is the use of thermoresponsive elastin-like peptides (ELPs) that consist of tandem repeats of the sequence VPGXG and precipitate with small temperature increases(4,5). ELPs undergo an inverse phase transition and aggregation, which is thought to be driven by the exposure of hydrophobic patches in the peptides upon heating (6). As part of a purification system, ELPs have been coupled to intein domains that have been genetically engineered into minimal self-cleaving units (7). When coupled, the ELP-intein system allows for a simple two-stage purification scheme. In the first step, precipitation of the ELP is triggered and the fusion protein is purified. Then, the intein is induced to cleave off the target protein and the ELP is again precipitated, leaving behind pure target protein in solution (8). While effective for many purification applications, the necessary heating of samples or the alternative use of high salt concentrations (9) can be problematic in many situations. Another protein-based non-chromatographic purification scheme developed by Ding et al. relies on calcium-dependent precipitation of an annexin B1 tag (10). As with ELPs, a self-cleaving intein is also incorporated in the fusion protein to remove the tag following purification.

Our interest in alternatives to chromatography for purifying proteins is a product of discoveries made while exploring repeat scaffolds for protein engineering applications. Repeat scaffolds are of interest to protein engineers as their repetitive, predictable secondary structures make them ideal for studying folding and engineering novel functions (11,12). There are examples of repeat scaffolds being engineered for biomolecular recognition, most notably the ankyrin repeats (13). In order to improve the engineerability of these scaffolds, efforts have been made at consensus design. Consensus design seeks to identify the core repeating peptide unit. Once this sequence is identified, multiple repeats can be concatenated as necessary for the desired application. Consensus design approaches have been successfully used for a number of repeat scaffolds, including ankyrin repeats, tetratricopeptide repeats, and armadillo repeats (14–17). The ability to alter the size of a scaffold is of particular use when engi-

Method summary:

A new calcium-responsive tag based on a consensus sequence found in the natural repeat-in-toxin (RTX) domain is presented. This calcium-responsive tag works under gentler reaction conditions than existing approaches and can be removed through protease cleavage, resulting in a pure, active target protein.

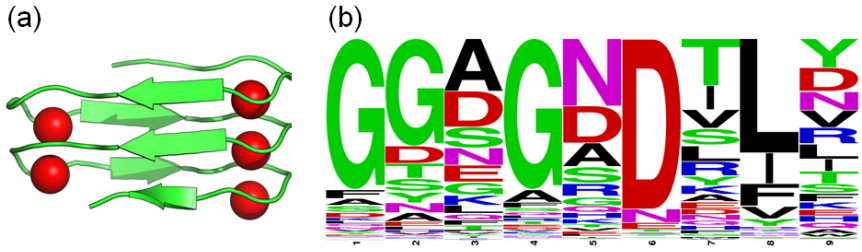

Figure 1. Beta roll structure and sequence logo. (a) Crystal structure of β roll domain from metalloprotease of S. marcescens (PDB: 1SAT). (b) Amino acid frequencies for single β roll repeat identifying consensus sequence GGAGNDTLY. Height of the letter corresponds to proportion of sequences containing the particular amino acid at that position. Sequence logo was generated using WebLogo (33,34).

neering binding, as the interface size can be tuned to the particular target.

In an effort to explore novel scaffolds for protein engineering, we have sought to identify a repeat scaffold that is also stimulus-responsive. To this end, we investigated the calcium-responsive repeat-in-toxin (RTX) domain. The RTX domain is found in proteins secreted through the bacterial type 1 secretion system (18). The domain consists of repeats of the consensus amino acid sequence GGXGXDXUX, where X is variable and U is a hydrophobic amino acid. One of the most well characterized RTX domains is the block V RTX domain from the adenylate cyclase toxin (CyaA) of *B. pertussis*. The domain is intrinsically disordered in the absence of calcium and forms a β roll structure (Figure 1A) in the presence of calcium (19). Of note, the block V RTX domain retains its reversible calcium-responsiveness even when expressed separately from the larger protein (20,21). Previous attempts have been made to use RTX domains in protein engineering, including incorporation into mesh networks, design of synthetic RTX peptides, and generation of hydrogel-forming RTX domains (22–25).

Our original objective was to design consensus RTX domains. Specifically, we identified the frequency of amino acids at each position of the nine amino acid repeat unit from a set of RTX-containing proteins (Figure 1B). This led to identification of the consensus sequence GGAGNDTLY. We then sought to create a library of consensus RTX constructs consisting of 5, 9, 13, or 17 repeats of the consensus unit. Upon purification of a number of these constructs, we observed that many of them precipitated in the presence of calcium. Therefore, we decided to explore the possibility of using these consensus β roll tags (BRTs) as a tools for bioseparation, similar to the ELP system. Here, we report the use of BRTs to purify recombinant proteins. We first purified a maltose binding protein (MBP)-BRT_{17} fusion as a proof of principle. Then, this MBP-BRT_{17} construct was fused to green fluorescent protein (GFP), which was used as a reporter during initial purification experiments. We have also fused β-lactamase and a thermostable alcohol dehydrogenase (AdhD) to demonstrate the feasibility of purifying enzymatic proteins. Finally, a specific protease site was engineered downstream of the tag to show that target proteins can be fully purified by protease cleavage while retaining their activity.

Materials and methods

Cloning

All cloning enzymes were purchased from New England Biolabs (Ipswich, MA). All oligonucleotides were synthesized by Integrated DNA Technologies (IDT) (Coralville, IA) and all sequences are available in Supplementary Table S1. Four differently sized MBP-BRT fusions were prepared consisting of 5, 9, 13, or 17 repeats of the consensus RTX sequence (named BRT_5, BRT_9, BRT_{13}, and BRT_{17}). In order to generate the DNA fragment for BRT_9, three oligonucleotides were synthesized: cons_β_1, cons_β_2, and cons_β_3. One ng each of these oligonucleotides was mixed along with the primers cons1_AvaI_F and cons9_BseRI_HindIII_R. PCR was performed and a clean product was obtained and gel extracted. This fragment was digested with *Ava*I and *Hin*dIII and cloned into the similarly digested pMAL_c4E vector to generate pMAL_BRT_9.

To generate the BRT_5 construct, pMAL_BRT_9 was used as a template for PCR with the primers cons1_AvaI_F and cons5_BseRI_HindIII_R. This product was digested with *Ava*I and *Hin*dIII and cloned into the pMAL_c4E vector producing pMAL_BRT_5.

BRT_{13} was produced by concatenation of four additional repeats to BRT_9. Concatenations were achieved using a recursive ligation technique we developed, similar to those previously described (26,27). This four repeat insert was amplified using primers cons1_BtsCI_F and cons4_BseRI_HindIII_R. The product was digested with *Bts*CI and *Hin*dIII and then cloned into pMAL_BRT_9 cut with *Bse*RI and *Hin*dIII to yield pMAL_BRT_{13}. BRT_{17} was produced analogously to BRT_{13}, except that the reverse primer cons8_BseRI_HindIII_R was used instead of cons4_BseRI_HindIII_R.

The *emGFP* gene was amplified from the Invitrogen pRSET/emGFP vector using primers GFP_BseRI_F and GFP_HindIII_R. The β-lactamase gene was amplified from the pMAL_c4E vector using primers βlac_BseRI_F and βlac_HindIII_R. The *AdhD* gene was amplified out of pWUR85 using primers AdhD_BserI_F and AdhD_HindIII_R (28). All three of these inserts were digested with *Bse*RI and *Hin*dIII and cloned into similarly digested pMAL_BRT_{17} to yield pMAL_BRT_{17}_GFP, pMAL_BRT_{17}_βlac and pMAL_ BRT_{17}_AdhD.

The native enterokinase site in the pMAL_c4E vector, which sits between MBP and BRT_{17}, was knocked out in the pMAL_BRT_{17}_βlac and pMAL_BRT_{17}_AdhD plasmids. Two rounds of site-directed mutagenesis were required to change the native recognition site, DDDDK, to DDGEQ, which was shown to be resistant to cleavage. A novel enterokinase recognition site was also engineered downstream of BRT_{17} in these constructs to allow for purification of the untagged protein of interest. Full plasmid maps of all cloned constructs are available in Supplementary Figure S1.

Expression and purification

For expression and cloning, Life Technologies (Grand Island, NY) Omnimax T1 E. coli cells were used. One L cultures of TB supplemented with 100 μg/mL ampicillin and 0.2% glucose were inoculated with 10 mL of overnight culture. Cultures were grown at 37°C with shaking at 225 RPM to an approximate OD600 of 0.5 and induced with 0.3 mM IPTG. Cells harboring pMAL_BRT_{17} and pMAL_BRT_{17}_βlac were allowed to express for an additional two hours and then harvested. Cultures transformed with pMAL_BRT_{17}_GFP were transferred to a shaker at 25°C and allowed to express for an additional 16 h and then harvested as no fluorescence was observed when expressed at 37°C. Cultures transformed with pMAL_BRT_{17}_AdhD were allowed to express at 37°C for an additional 16 h as previously reported (28). Cells were harvested after expression and resuspended in 1/20 culture volume of 50 mM tris-HCl, pH 7.4 for precipitation purification. For amylose resin purification, cells were resuspended in 1/20 culture volume of MBP column buffer (20 mM tris-HCl, 200 mM NaCl, 1 mM EDTA, pH 7.4). In both cases, cells were subsequently lysed via

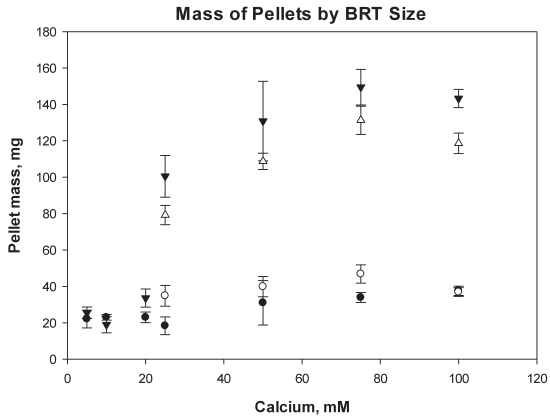

Figure 2. Role of BRT length in precipitation. Mass of precipitated pellet vs. calcium chloride concentration and BRT size. Results for MBP-BRT_5(●), MBP-BRT_9(○), MBP-BRT_{13}(▼), and MBP-BRT_{17}(△). Error bars represent standard deviations for 3 trials.

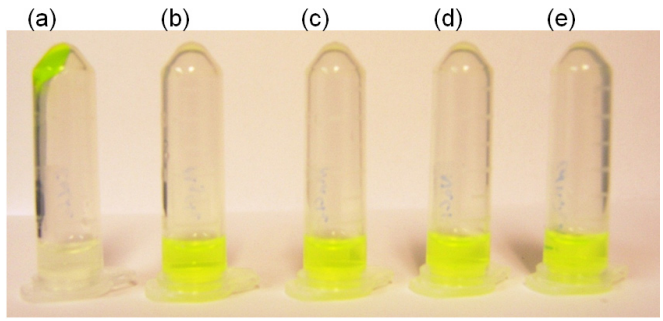

Figure 3. Ion specificity of BRT precipitation. Purified MBP-BRT_{17}-GFP was mixed with 100 mM of the compound indicated, and centrifuged to collect any pellet. The tube was then inverted so that precipitated protein remained on top. The compounds were as follows: (a) $CaCl_2$, (b) $MgCl_2$, (c) $MnCl_2$, (d) NaCl, and (e) $(NH_4)_2SO_4$

sonication using 15 s pulses for a total of 150 s. Lysate was then clarified by centrifugation at 15,000 g for 30 min at 4°C. For amylose resin purification, clarified lysate was diluted with five volumes of column buffer and purified as previously described (21). All subsequent steps were performed at room temperature.

For precipitation purification, clarified lysate was added to a concentrated calcium stock according to the data presented in Figure 2. For example, for precipitation of MBP-BRT_{17} lysate in 100 mM CaCl2, 950 µL of clarified lysate was added to 50 µL of 2 M CaCl2 solution. The sample was promptly mixed by gentle pipetting, allowed to sit at room temperature for 2 min and then centrifuged at 16,000 g in a microcentrifuge for 2 min. The supernatant was carefully removed and the pellet was resuspended in the same tris buffer by gentle pipetting. The turbid solution was centrifuged and washed for four additional cycles. For the final step, the pellet was resuspended in tris buffer with a concentration of EGTA equivalent to the original calcium concentration. Gentle pipetting was sufficient to cause the sample to redissolve as confirmed by observation and the lack of a precipitate upon subsequent centrifugation.

All chemicals were obtained from Sigma Aldrich (St. Louis, MO), unless otherwise specified.

Recovery, activity, and fluorescence assays

Concentrations of all purified proteins were determined by 280 nm absorbance using extinction coefficients predicted by ExPASy (www.expasy.org). All extinction coefficients are provided in Supplementary Table S2. Recovery of MBP-BRT_{17} by either amylose resin purification or precipitation was determined solely using this method.

MBP-BRT_{17}-GFP recoveries were estimated by comparing fluorescence emission intensity at 509 nm with excitation at 487 nm. 100-fold dilutions of both clarified lysate and purified protein were made for fluorescence measurements. Purified proteins were resuspended in the same volume as the lysate from which they were extracted, so signals were compared directly.

For estimation of MBP-BRT_{17}-βlac recovery, protein was added to a nitrocefin solution and the absorbance at 486 nm was tracked corresponding to the hydrolysis of nitrocefin. 500 µL of nitrocefin solution was prepared by placing three nitrocefin disks (Fluka) in 450 µL 50 mM tris-HCl, pH 7.4 and 50 µL DMSO. In each sample well, 50 µL of this solution was mixed with 90 µL of the same tris buffer and 10 µL of protein sample. For each sample tested, serial dilutions from 1X to 1000X were prepared from lysate and purified protein. Initial rates were determined by measuring the change in absorbance at 486 nm over the first 20% of the change in signal between the starting absorbance and the end absorbance. The same nitrocefin stock solution was used for all samples to account for variations in concentration.

MBP-BRT_{17}-AdhD recovery was also evaluated by enzymatic activity using a protocol previously described (28). Since this AdhD was isolated from the hyperthermofile *Pyrococcus furiosus*, all samples were heat treated at 80°C for 1 h prior to evaluating activity. All assays were performed at saturated conditions of both cofactor and substrate, 0.5 mM NAD+ and 100 mM 2,3-butanediol, respectively. Reaction mixtures containing 2,3-butanediol and protein sample in 50 mM glycine pH 8.8 were incubated at 45°C in a 96 well UV microplate in a spectrophotometer. Reactions were initiated by the addition of NAD+. Initial rates were calculated by following the production of NADH at 340 nm. Specific activity of cleaved AdhD was calculated using an NADH extinction coefficient (ε = 6.22 mM-1 cm-1).

All spectroscopic measurements were done on a SpectraMax M2 (Molecular Devices; Sunnyvale, CA).

Results and discussion

In order to identify the consensus RTX sequence, a database of RTX containing proteins was constructed by searching the UniProt (www.uniprot.org) database for hemolysin-type calcium binding domains. Individual repeats were identified and the frequency of amino acids at each of the nine repeat positions was determined (Figure 1B). From this result, the repeat sequence GGAGNDTLY was identified as the consensus sequence. For a few of these positions, other amino acids were found with nearly equal frequency. However, as this sequence was found to be effective for purification, further investigation on sequence variation was not performed. A variety of synthetic RTX domains of different lengths (BRT_5, BRT_9, BRT_{13}, BRT_{17}) were prepared as fusions to the C terminus of MBP, with subscripts denoting the number of repeats. These lengths were chosen as they reflect the variability of naturally occurring RTX domains. Unexpectedly, we observed that upon the addition of calcium to the purified BRT_{17} construct, there was significant precipitation out of solution, which was reversed upon the addition of the chelating agent EGTA.

In order to more thoroughly characterize the observed precipitation behavior, cells were induced to express the four MBP-BRT constructs. Clarified cell lysates were

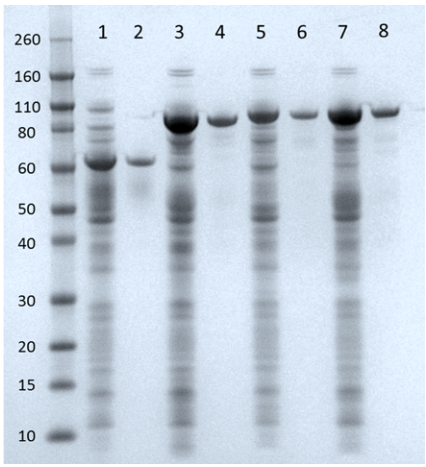

Figure 4. SDS-PAGE results for purification of the four constructs tested. Numbers are standard size in kDa. Expected molecular weights for MBP-BRT_{17}, MBP-BRT_{17}-GFP, MBP-BRT_{17}-βlac, and MBP-BRT_{17}-AdhD are 57.1, 83.4, 88.6, and 89.1 kDa, respectively. (1–2) Purification of MBP-BRT_{17}. Lane 1 is clarified lysate, and Lane 2 is purified fusion protein. (3–4) Same samples for purification of MBP-BRT_{17}-GFP. (5–6) Same samples for MBP-BRT_{17}-βlac. (7–8) Same samples for MBP-BRT_{17}-AdhD.

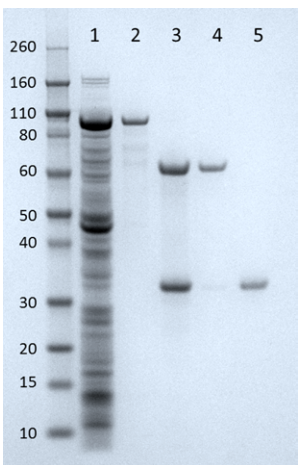

Figure 5. SDS-PAGE results for purification and cleavage of AdhD. Numbers are standard size in kDa. Estimated molecular weight for AdhD is 31.9 kDa. (1) Clarified MBP-BRT_{17}-AdhD lysate. (2) Purified fusion protein. (3) Enterokinase cleavage. (4) Precipitated MBP-BRT_{17}. (5) Soluble AdhD. 3x protein concentrations were used in lanes 3, 4, and 5.

prepared from these four cultures and then titrated with calcium to assess precipitation behavior by mixing with $CaCl_2$ solution at the indicated concentrations, followed by by centrifugation, and measurement of the mass of the pellet (Figure 2). Due to possible variations in cell growth rates and densities, all cultures were started from saturated overnight cultures and induced simultaneously. Both BRT_{13} and BRT_{17} precipitated when calcium concentrations exceeded 25 mM. Some precipitation was observed from BRT_5 and BRT_9 lysate, similar to what was observed with control cell lysate. Addition of an equivalent concentration of EGTA allowed the pellets to quickly dissolve again upon gentle pipetting.

While both BRT_{13} and BRT_{17} precipitated upon calcium addition, BRT_{17} formed a pellet that was easier to clarify and was therefore selected for further examination. Three additional constructs were prepared by fusing MBP-BRT_{17} to the N terminus of GFP, β-lactamase, and AdhD (named MBP-BRT_{17}-GFP and MBP-BRT_{17}-βlac, MBP-BRT_{17}-AdhD respectively). These three proteins were fused to MBP to allow for amylose resin chromatography purification as a comparison technique. GFP was chosen as a reporter protein for initial purification experiments to track the location of the BRT. β-lactamase and AdhD were chosen as they are well characterized enzymes whose activity can be measured with straightforward assays.

The folding of RTX domains into β rolls is highly calcium specific. Therefore, we were interested in whether or not the precipitation behavior observed was also calcium-specific. To test this, MBP-BRT_{17}-GFP was purified on an amylose resin and diafiltered into salt-free tris buffer. Diafiltration was necessary as proteins are purified in high salt buffer for the amylose resin step and it was observed that BRT precipitation was significantly reduced in high salt. This is consistent with previous observations that RTX calcium affinity is reduced with increasing salt concentration (29). Solutions of various salts were added to final concentrations of 100 mM. The samples were then gently mixed by pipetting, allowed to sit for 2 min, and centrifuged at 16,000 g in a microcentrifuge for 2 min. Tubes were then inverted and the presence of a pellet at the top was indicative of precipitation (Figure 3). BRT precipitation was observed to be calcium-specific, with near complete precipitation of MBP-BRT_{17}-GFP (as indicated by the remaining color in solution) in the presence of calcium and no precipitation with other salts. While this behavior does not establish the formation of a β roll structure, it does indicate that at least one property of the β roll is preserved in these constructs.

For all 4 constructs tested, calcium concentrations greater than 25 mM were found to cause precipitation of the fusion protein. To assess the ideal calcium concentration, all 4 constructs were precipitated from 1 mL of clarified cell lysate in 25, 50, 75, and 100 mM $CaCl_2$. Pellets were washed in salt-free tris buffer five times. Pellets were broken up upon washing, but did not redissolve until exposed to an equivalent concentration of EGTA after the final wash. The 100 mM $CaCl_2$ samples were found to not fully redissolve, so only lower $CaCl_2$ concentrations were tested further. A slight increase in recovery was observed at 75 mM $CaCl_2$ (as compared with lower $CaCl_2$ concentrations) as confirmed by SDS-PAGE (data not shown). All 4 constructs were subsequently purified by precipitation with 75 mM $CaCl_2$ and SDS-PAGE gels were run after 5 washes (Figure 4). No significant difference was found with increasing number of washes, so further quantification and recovery measurements were performed on samples washed five times. To confirm scalability, the analogous protocol was also performed on 50 mL lysate, and comparable results were obtained (data not shown). Additionally, we briefly tested the reversibility of the precipitation process. It was found that addition of calcium to the redissolved pellet in EGTA solution did yield a pellet once again. Full pellet size was only recovered after dialysis into EGTA-free buffer.

We next sought to quantify the recovery and functionality of the purified proteins after precipitation. To assess recovery of MBP-BRT_{17}, we used the theoretically determined extinction coefficient to estimate concentration by absorbance at 280 nm (30). Results from purifying the construct on an amylose resin were compared with BRT precipitation. For MBP-BRT_{17}-GFP,

Table 1 Recovery data for three constructs tested.

	MBP-BRT_{17}	MBP-BRT_{17}-GFP		MBP-BRT_{17}-βlac		MBP-BRT_{17}-AdhD	
Calcium, mM	Fold versus Resin	Fold versus Resin	Fluorescence	Fold versus Resin	Activity Recovered	Fold versus Resin	Activity Recovered
25	2.0 ± 0.1	2.8 ± 0.1	61 ± 3%	4.1 ± 0.1	1.6 ± 0.1%	1.6 ± 0.1	3.8 ± 0.5%
50	2.3 ± 0.1	3.7 ± 0.1	86 ± 6%	5.3 ± 0.2	4.0 ± 0.1%	1.7 ± 0.1	4.7 ± 0.7%
75	2.2 ± 0.2	2.8 ± 0.3	78 ± 8%	5.1 ± 0.2	3.4 ± 0.1%	2.2 ± 0.1	8.3 ± 1.4%

"Fold versus Resin" denotes protein quantity recovered relative to amylose resin for equivalent loading amount. For MBP-BRT_{17}-GFP, MBP-BRT_{17}- βlac, and MBP-BRT_{17}-AdhD fluorescence and activity are the respective properties relative to clarified lysate. Errors represent standard deviations. All data were collected in triplicate.

recoveries were calculated as the percentage of fluorescence signal of purified sample compared with lysate (this was normalized against control lysate). Along with total protein recoveries estimated by UV absorbance, recoveries of both MBP-BRT_{17}-βlac and MBP-BRT_{17}-AdhD were estimated by comparing lysate activity to the activity of these constructs after purification. MBP-BRT_{17}-βlac recoveries were calculated using activity measured by tracking the absorbance at 486 nm for the hydrolysis of nitrocefin. MBP-BRT_{17}-AdhD recoveries were calculated by tracking NADH formation at 340 nm in saturating conditions of both substrate and cofactor. Results of these trials are shown in Table 1. For MBP-BRT_{17}, calcium precipitation recovers about double the amount of protein as compared with amylose resin purification. For MBP-BRT_{17}-GFP, we observed up to 86% recovery of fluorescence. MBP-BRT_{17}-βlac recovery from the lysate was not as high, but was still 5-fold better than the amylose resin, yielding a significant quantity of protein. Similar results were also observed for MBP-BRT_{17}-AdhD, although the yields were not quite as high compared with the resin (2-fold improvement). It should be noted that while the overall values of the activities recovered in Table 1 appear low, they were all larger than the values obtained using the amylose resin purification. It is also possible that measuring activity in crude extracts may introduce error beyond what was accounted for in the measurement of endogenous hydrolysis (β-lactamase) and reduction (AdhD). Table 2 lists the absolute yield of each fusion protein based on UV absorption at 280 nm. All fusion proteins were shown to be purified in high yields.

To increase the utility of this tag, it would be beneficial to couple our system with a cleavage tag to separate the protein of interest from the BRT. The pMAL_c4E vector we used for these experiments contains a cleavable enterokinase site between the MBP and BRT. This recognition sequence was removed via site-directed mutagenesis. A new enterokinase site was engineered between the BRT and the protein of interest for MBP-BRT_{17}-βlac and MBP-BRT_{17}-AdhD. Therefore, as a proof of principle, we took precipitation purified MBP-BRT_{17}-βlac and MBP-BRT_{17}-AdhD and subjected them to overnight cleavage by enterokinase digestion. Calcium can then be added directly to the cleavage reaction to precipitate MBP-BRT_{17}, thereby separating the tag from the protein of interest following centrifugation. This is shown in Figure 5 for MBP-BRT_{17}-AdhD, showing pure, soluble protein by SDS-PAGE. Recoveries of 93 ± 7% were obtained by tracking UV absorbance at 280 nm, meaning 93% of the AdhD in the precipitation purified sample was recovered after cleavage and reprecipitation of the tag. Specific activity of the purified enzyme was also calculated to be 20.2 ± 1.3 min^{-1}, which is similar to what has been previously reported, indicating this system has little to no effect on the activities of purified proteins (28). However, in the case of MBP-BRT_{17}-βlac, the cleaved β-lactamase remained in the insoluble fraction following enterokinase cleavage and calcium precipitation. Upon further investigation it was found that β-lactamase will precipitate in high calcium concentrations. As a control experiment, we purchased recombinant β-lactamase and observed similar behavior. In 75mM $CaCl_2$, an insoluble pellet was formed upon centrifugation. Activity assays confirmed a significant amount of active protein in the insoluble fraction (data not shown). This illustrates a caveat of the BRT system. Proteins that naturally precipitate in $CaCl_2$ solutions cannot be efficiently separated from the BRT. For future improvement of this system, the protease used could be fused to the precipitating BRT or a self-cleaving intein could be incorporated. Fusing the protease to the BRT would enable its removal from the target protein in the final precipitation. A self-cleaving intein would fulfill a similar function. It should also be noted that the BRT can precipitate without being fused to the MBP, suggesting that the MBP is not essential for this system; however, the MBP may be useful for improving protein expression levels.

Table 2 Absolute fusion protein yields.

	Absolute Yield (mg/L)			
Calcium, mM	MBP-BRT_{17}	MBP-BRT_{17}-GFP	MBP-BRT_{17}- βlac	MBP-BRT_{17}-AdhD
25	268 ± 11	333 ± 12	124 ± 3	198 ± 3
50	305 ± 14	434 ± 17	160 ± 7	273 ± 9
75	295 ± 26	336 ± 40	176 ± 5	214 ± 6

Amount of protein recovered for each fusion construct after precipitation and washing. Values were determined using UV absorbance at 280 nm and calculated extinction coefficients available in the Supplementary Table S2. All data were collected in triplicate and errors represent standard deviations.

It is not completely clear why these consensus RTX constructs are able to function as bioseparation tags. We do observe a correlation between length and precipitation (Figure 2), so size certainly plays a role. However, there has not been extensive work in studying the role of the number of repeats on RTX behavior. We recently studied the impact of altering the number of native RTX repeats in the block V CyaA RTX domain of *B. pertussis* but no significant size effect was observed and, furthermore, C-terminal capping was required for calcium-responsiveness (31). As for past efforts to design synthetic RTX domains, the synthetic domains created by Scotter et al. consisted of 4 RTX repeats and those prepared by Lilie et al. consisted of 8 repeats (22,24). The peptides create by Lilie et al. were weakly calcium-responsive, while those of Scotter et al. were only lanthanum-responsive and formed partially insoluble filaments in the presence of lanthanum. In general, it is fairly well established that β sheets are prone to aggregation and nature uses various strategies to ensure solubility of proteins containing these motifs (32), so perhaps BRTs are a balance between this tendency and the calcium-responsiveness of the β roll. Further investigation will be required to better elucidate the mechanism of BRT functionality, but their use as a tool for protein purification is clear.

The technique described here offers a new stimulus-responsive phase-changing peptide that could be useful in a range of applications similar to those for which ELPs have been used, such as recombinant protein purification or the creation of "smart" biomaterials. This new tag possesses certain advantages over ELPs and annexin B1 since precipitation is simpler to achieve and the BRT peptide is significantly smaller. Additionally, BRT_{17} precipitates in as little as 25 mM $CaCl_2$ at room temperature, compared to the larger ionic strength and higher temperature increases required for ELP precipitation. Precipitation also occurs instantaneously, whereas annexin B1-based systems require a 2 h incubation period at 4°C. Overall, BRTs offer a new tool for rapid purification of recombinant proteins. The protocol described here can be performed to obtain purified fusion protein from lysate in only a few minutes. Further optimization of the BRT system should enable the use of specific proteases to purify target proteins and further improve the precipitation and resolubilization process, greatly enhancing the ability to rapidly purify recombinant proteins.

Acknowledgements

The authors gratefully acknowledge funding from the National Science Foundation.

Competing interests

The authors declare no competing interests.

References

1. **Przybycien, T.M., N.S. Pujar, and L.M. Steele.** 2004. Alternative bioseparation operations: life beyond packed-bed chromatography. Curr. Opin. Biotechnol. *15*:469-478.
2. **Balan, S., J. Murphy, I. Galaev, A. Kumar, G.E. Fox, B. Mattiasson, and R.C. Willson.** 2003. Metal chelate affinity precipitation of RNA and purification of plasmid DNA. Biotechnol. Lett. *25*:1111-1116.
3. **Kumar, A., P.O. Wahlund, C. Kepka, I.Y. Galaev, and B. Mattiasson.** 2003. Purification of histidine-tagged single-chain Fv-antibody fragments by metal chelate affinity precipitation using thermoresponsive copolymers. Biotechnol. Bioeng. *84*:494-503.
4. **McPherson, D.T., J. Xu, and D.W. Urry.** 1996. Product purification by reversible phase transition following Escherichia coli expression of genes encoding up to 251 repeats of the elastomeric pentapeptide GVGVP. Protein Expr. Purif. *7*:51-57.
5. **Meyer, D.E. and A. Chilkoti.** 1999. Purification of recombinant proteins by fusion with thermally-responsive polypeptides. Nat. Biotechnol. *17*:1112-1115.
6. **Yamaoka, T., T. Tamura, Y. Seto, T. Tada, S. Kunugi, and D.A. Tirrell.** 2003. Mechanism for the phase transition of a genetically engineered elastin model peptide (VPGIG)40 in aqueous solution. Biomacromolecules *4*:1680-1685.
7. **Wood, D.W., W. Wu, G. Belfort, V. Derbyshire, and M. Belfort.** 1999. A genetic system yields self-cleaving inteins for bioseparations. Nat. Biotechnol. *17*:889-892.
8. **Banki, M.R., L. Feng, and D.W. Wood.** 2005. Simple bioseparations using self-cleaving elastin-like polypeptide tags. Nat. Methods *2*:659-661.
9. **Fong, B.A., W.Y. Wu, and D.W. Wood.** 2009. Optimization of ELP-intein mediated protein purification by salt substitution. Protein Expr. Purif. *66*:198-202.
10. **Ding, F.X., H.L. Yan, Q. Mei, G. Xue, Y.Z. Wang, Y.J. Gao, and S.H. Sun.** 2007. A novel, cheap and effective fusion expression system for the production of recombinant proteins. Appl. Microbiol. Biotechnol. *77*:483-488.
11. **Courtemanche, N. and D. Barrick.** 2008. The leucine-rich repeat domain of Internalin B folds along a polarized N-terminal pathway. Structure *16*:705-714.
12. **Grove, T.Z., A.L. Cortajarena, and L. Regan.** 2008. Ligand binding by repeat proteins: natural and designed. Curr. Opin. Struct. Biol. *18*:507-515.
13. **Binz, H.K., P. Amstutz, A. Kohl, M.T. Stumpp, C. Briand, P. Forrer, M.G. Grutter, and A. Pluckthun.** 2004. High-affinity binders selected from designed ankyrin repeat protein libraries. Nat. Biotechnol. *22*:575-582.
14. **Mosavi, L.K., T.J. Cammett, D.C. Desrosiers, and Z.Y. Peng.** 2004. The ankyrin repeat as molecular architecture for protein recognition. Protein Sci. *13*:1435-1448.
15. **Main, E.R., Y. Xiong, M.J. Cocco, L. D'Andrea, and L. Regan.** 2003. Design of stable alpha-helical arrays from an idealized TPR motif. Structure *11*:497-508.
16. **Parmeggiani, F., R. Pellarin, A.P. Larsen, G. Varadamsetty, M.T. Stumpp, O. Zerbe, A. Caflisch, and A. Pluckthun.** 2008. Designed armadillo repeat proteins as general peptide-binding scaffolds: Consensus design and computational optimization of the hydrophobic core. J. Mol. Biol. *376*:1282-1304.
17. **Binz, H.K., M. Stumpp, P. Forrer, P. Amstutz, and A. Plückthun.** 2003. Designing repeat proteins: well-expressed, soluble and stable proteins from combinatorial libraries of consensus ankyrin repeat proteins. J. Mol. Biol. *332*:489-503.
18. **Holland, I.B., L. Schmitt, and J. Young.** 2005. Type 1 protein secretion in bacteria, the ABC-transporter dependent pathway review. Mol. Membr. Biol. *22*:29-39.
19. **Chenal, A., J.I. Guijarro, B. Raynal, M. Delepierre, and D. Ladant.** 2009. RTX calcium binding motifs are intrinsically disordered in the absence of calcium: implication for protein secretion. J. Biol. Chem. *284*:1781-1789.
20. **Bauche, C., A. Chenal, O. Knapp, C. Bodenreider, R. Benz, A. Chaffotte, and D. Ladant.** 2006. Structural and functional characterization of an essential RTX subdomain of *Bordetella pertussis* adenylate cyclase toxin. J. Biol. Chem. *281*:16914-16926.
21. **Blenner, M.A., O. Shur, G.R. Szilvay, D.M. Cropek, and S. Banta.** 2010. Calcium-induced folding of a beta roll motif requires C-terminal entropic stabilization. J. Mol. Biol. *400*:244-256.
22. **Lilie, H., W. Haehnel, R. Rudolph, and U. Baumann.** 2000. Folding of a synthetic parallel beta-roll protein. FEBS Lett. *470*:173-177.
23. **Ringler, P. and G.E. Schulz.** 2003. Self-assembly of proteins into designed networks. Science *302*:106-109.
24. **Scotter, A.J., M. Guo, M.M. Tomczak, M.E. Daley, R.L. Campbell, R.J. Oko, D.A. Bateman, A. Chakrabartty, et al.** 2007. Metal ion-dependent, reversible, protein filament formation by designed beta-roll polypeptides. BMC Struct. Biol. *7*:63.
25. **Dooley, K., Y.H. Kim, H.D. Lu, R. Tu, and S. Banta.** 2012. Engineering of an Environmentally Responsive Beta Roll Peptide for Use As a Calcium-Dependent Cross-Linking Domain for Peptide Hydrogel Formation. Biomacromolecules *13*:1758-1764.
26. **Meyer, D.E. and A. Chilkoti.** 2002. Genetically encoded synthesis of protein-based polymers with precisely specified molecular weight and sequence by recursive directional ligation: Examples from the elastin-like polypeptide system. Biomacromolecules *3*:357-367.
27. **McDaniel, J.R., J.A. MacKay, F.G. Quiroz, and A. Chilkoti.** 2010. Recursive Directional Ligation by Plasmid Reconstruction Allows Rapid and Seamless Cloning of Oligomeric Genes. Biomacromolecules *11*:944-952.
28. **Campbell, E., I.R. Wheeldon, and S. Banta.** 2010. Broadening the cofactor specificity of a thermostable alcohol dehydrogenase using rational protein design introduces novel kinetic transient behavior. Biotechnol. Bioeng. *107*:763-774.
29. **Szilvay, G.R., M.A. Blenner, O. Shur, D.M. Cropek, and S. Banta.** 2009. A FRET-based method for probing the conformational behavior of an intrinsically disordered repeat domain from Bordetella pertussis adenylate cyclase. Biochemistry *48*:11273-11282.
30. **Gill, S.C. and P.H. Vonhippel.** 1989. Calculation of Protein Extinction Coefficients from Amino-Acid Sequence Data. Anal. Biochem. *182*:319-326.
31. **Shur, O. and S. Banta.** 2012. Rearranging and concatenating a native RTX domain to understand sequence modularity. Protein Engineering Design and Selection.
32. **Richardson, J.S. and D.C. Richardson.** 2002. Natural beta-sheet proteins use negative design to avoid edge-to-edge aggregation. Proc. Natl. Acad. Sci. USA *99*:2754-2759.
33. **Crooks, G.E., G. Hon, J.M. Chandonia, and S.E. Brenner.** 2004. WebLogo: A sequence logo generator. Genome Res. *14*:1188-1190.
34. **Schneider, T.D. and R.M. Stephens.** 1990. Sequence Logos - a New Way to Display Consensus Sequences. Nucleic Acids Res. *18*:6097-6100.

Received 27 June 2012; accepted 13 March 2013

Address correspondence to Scott Banta, Department of Chemical Engineering, Columbia University, New York, New York. E-mail: sbanta@columbia.edu